ELSEVIER

International Journal of Solids and Structures 41 (2004) 607–618

INTERNATIONAL JOURNAL OF SOLIDS and STRUCTURES

www.elsevier.com/locate/ijsolstr

On the path dependence of the J-integral in notch problems

Yi-Heng Chen [a], Tian Jian Lu [b,*]

[a] School of Civil Engineering and Mechanics, Xi'an Jiaotong University, 710049, PR China

[b] Department of Engineering, University of Cambridge, Trumpington Street, Cambridge CB2 1PZ, UK

Received 25 September 2003; received in revised form 25 September 2003

Abstract

This study attempts to clarify the conditions under which the J-integral is path-independent in U- and V-shaped notch problems. The key is to determine the contribution to the J-integral evaluated in the global coordinate system from the second component of the J_k-vector evaluated in the local coordinate system along the traction-free surfaces that form part of the integration path. It is found that the global J-integral is path-independent only if the projected contribution from the J_2-integral to J vanishes. The J-integral for a V-shaped notch is, strictly speaking, path-dependent even under remote symmetrical loading. This is due to the fact that, unlike in the case of a line- or plane-crack, the value of the J-integral calculated along a closed contour surrounding the V-shaped notch is dependent on the selection of the starting and ending points on the notch surface. In other words, the traction-free surface of the V-shaped notch does contribute to the J-integral due to the non-zero projected values induced from the J_2-integral.

For a U-shaped notch, the path-independence of the J-integral is established if the integration path completely encloses the notch root. This is because both the upper and lower notch surfaces of the U-shaped notch are parallel to the geometric symmetrical line (the x_1-axis) and hence the projected values from the J_2-integral vanish. Furthermore, it is found that the small arc at the root of the notch (whether U- or V-shaped) also contributes to the J-integral even if the remote loading is symmetrical. These conclusions are derived by detailed analytical manipulations and by numerical examples; the analytical solution obtained by Lazzarin and Tovo [Int. J. Fracture 78 (1996) 3] and Lazzarin et al. [Int. J. Fracture 91 (1998) 269] for stress field in the vicinity of a notch root in an infinite elastic plane is used to calculate the contribution induced from the arc with different radii. Some useful results for studying the fracture and fatigue of notches are discussed.

Keywords: J-integral; Path-independence; Notch and crack; Analytical modeling; Numerical simulation

1. Introduction

The ability to assess and forecast the service life of structural components containing highly stress concentrated notch-like defects is of great practical significance. There have been a number of investigations aiming at predicting the fatigue life after crack initiation commences from a notch: recent contributions in

* Corresponding author. Tel.: +44-1223766316; fax: +44-1223332662.

E-mail addresses: yhchen2@xjtu.edu.cn (Y.-H. Chen), tjl21@eng.cam.ac.uk (T.J. Lu).

0020-7683/$ - see front matter © 2003 Elsevier Ltd. All rights reserved.
doi:10.1016/j.ijsolstr.2003.10.007

this field include Kujawski (1991), Shin et al. (1994), Xu et al. (1995), Lazzarin and Tovo (1996), Lazzarin et al. (1998), Atzori et al. (1997), and Kujawski and Shin (1997). However, all these studies focus either on how to calculate stress concentration factors and the associated stress distributions ahead of the notch before crack initiation has occurred (from which the degree of accuracy for predicting fatigue crack initiation and subsequent crack propagation could be ensured), or on how to measure crack-growth resistance curves (i.e., R curves) from notch specimens.

The path-independence of J-integral for plane cracks is well-known and widely exploited for studying fracture in both linear and non-linear elastic materials (Rice, 1968a,b; Eshelby, 1970). This integral has also been applied in situations where the crack is blunt (i.e., U- or V-shaped notches). Some major contributions in this field can be found in the works by Blackburn (1972, 1977), Hutchinson (1979), McMeeking (1980), Elhaddad et al. (1980), Atluri (1982), Castro (1982), Ranaweera and Leckie (1982), Batte et al. (1983), Sinclair and Mullan (1982), Sinclair et al. (1984), Kanninen and Popelar (1985), and Glinka and Newport (1987). These studies directly lead to the ASTM Standards (1990) for measuring R curves based on notch specimens. However, the necessary conditions of the J-integral application, under which its path-independence is valid, have received little attention.

Generally speaking, the widely recognized view regarding the use of the J-integral is that the traction-free surfaces of a crack (or notch) does not yield any contribution to the integral evaluated along an arbitrarily selected close contour originating from a point on the lower crack (notch) surface and extending counterclockwise around the crack (notch) tip to a point on the upper surface (see, e.g., Kanninen and Popelar, 1985). In other words, the value of J does not depend on the selection of the starting and ending points of the integration path. However, to the authors' best knowledge, there appears to be no detailed account of the necessary conditions under which the path-independence of the J-integral is ensured. Evidences cited in this paper reveal that these conditions are sometimes overlooked (apart from the known necessary condition that the stress path should be proportional or nearly proportional in the material), which may lead to the misinterpretation or even incorrect use of the integral.

To proceed forward, we note that the J-integral as proposed by Rice (1968a,b) is only the first component of a vector J_k $(k = 1, 2)$, representing the component of the vector in the direction parallel to the x_1-axis (here and below, the x_1-axis is customarily chosen along the geometrical symmetrical line of a notch or a crack). For a single plane crack, the J_k-vector is given by (Knowles and Sternberg, 1972; Budiansky and Rice, 1973):

$$J_k = \oint_{\mathrm{Co}} (w n_k - u_{i,k} T_i)\,\mathrm{d}s \quad (k = 1, 2) \tag{1}$$

where w denotes strain energy density, n_k is unit outward normal vector to the closed contour Co, and u_i, T_i are displacement and traction vectors, respectively. The second component, J_2, is less popular than $J(\equiv J_1)$ due to its path-dependence nature (Herrmann and Herrmann, 1981). The closed path Co is chosen such that it surrounds one crack tip and does not enclose the other tip (or other singularities). Otherwise, if the path Co encloses the crack completely, the trivial result $J_1 = J_2 = 0$ holds (Herrmann and Herrmann, 1981). Recent investigations show that $J_1 = J_2 = 0$ is still valid even when Co encloses strongly-interacting multiple cracks, so long as there is no other singularity outside Co and the projected values induced from both components of the vector are taken into account (Chen and Hasebe, 1998).

Two typical notch problems are analyzed in this paper, one associated with the V-shaped notches and the other with the U-shaped notches. For simplicity, notches embedded in two-dimensional, infinitely large solids are considered (Fig. 1). Detailed manipulations (Section 2) and numerical calculations (Section 3) are presented to show that caution must be taken when applying the J-integral in notch problems. It will be demonstrated that the traction-free surfaces of a notch could not always ensure the path-independence of J, if the surfaces are partially or entirely inclined (or curved) with respect to the global x_1-axis (i.e., the symmetrical line of the notch). It is found that J is path-independent for a U-shaped notch if the notch root

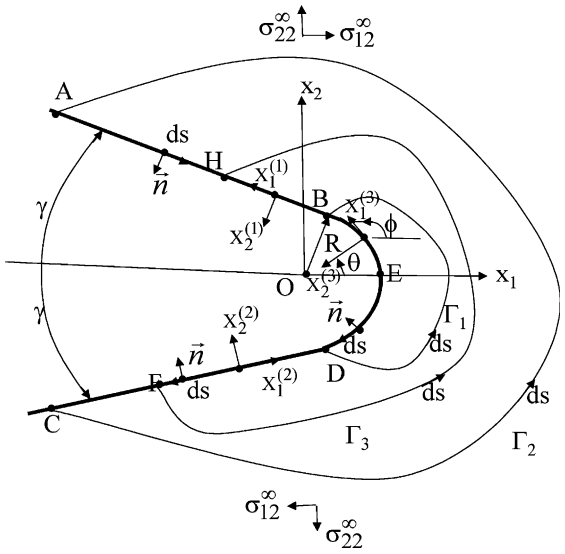

Fig. 1. Notations and coordinate systems for a notch subjected to combined opening and shear loading at remote.

is completely enclosed by the selected integration path, and always path-dependent for a V-shaped notch. For the latter, the J_2-integral evaluated in a local system that traverses along the inclined surface has a non-vanishing projected value on the global x_1-axis, causing the J-integral to be dependent upon the selection of the starting and ending points of the integration path on notch surfaces. Furthermore, the traction-free arc at the root of a V- or U-shaped notch always contributes to the J-integral, as a result of the projected value induced from the J_2-integral.

2. A notch under remote mixed-mode loading

The purpose of this section is not to deal with crack initiation and fatigue problems associated with notches, but to provide the necessary conditions under which the path-independence of the J-integral is valid. Special attention is directed at clarifying the important role of the J_2-integral in notch-like problems.

With reference to Fig. 1, consider a V-shaped notch (i.e., a blunt crack) defined by a small circular arc $\overset{\frown}{DEB}$, radius R and centered at the origin O of the global coordinate system (x_1, x_2) and two straight segments $\overline{AB}$ and $\overline{CD}$ inclined at an angle $\pm\gamma$ with respect to the x_1-axis. A U-shaped notch is defined as the special case of the V-notch with $\gamma = 0$. Tensile stress σ_{22}^{∞} and shear stress σ_{12}^{∞} are applied at remote, perpendicular and parallel to the geometric symmetric line of the notch, respectively. Three different closed contours Γ_1, Γ_2 and Γ_3 are introduced in Fig. 1, originating separately from points D, C, and F on the lower surface of the notch and ending at points B, A, and H on the upper surface. The length of $\overline{AB}$ equals that of $\overline{CD}$, but $\overline{HB}$ has a length different from that of $\overline{FD}$.

Because the J-integral is widely accepted as path-independent, one may customarily assert that J evaluated along the above three closed contours should have identical values. For instance, some manipulations and applications of J for a blunt crack were performed (see, e.g., McMeeking, 1980), and a test method for determining the R curves from notch specimens was standardized by ASTM (1990). However, as demonstrated below, this assertion has been based on the condition that the traction-free notch surfaces, i.e., arc $\overset{\frown}{DEB}$ plus the two inclined straight segments, do not contribute to J $(\equiv J_1)$ defined in the global

system. In fact, whether or why the basic condition is satisfied remains unclear since the role of the second component of the J_k-vector, J_2, in blunt crack problems is yet to be clarified.

Whilst J_2 is in general path-dependent, it will be shown next that the path-independence of J is only conditional, which should be used with caution when extrapolated to situations where the basic condition may be violated. To calculate J for a blunt crack (Fig. 1), consider first the contribution of segment $\overline{AB}$ and denote it by J_{AB} in the global coordinate system (x_1, x_2). From (1), it follows that:

$$J_{AB} = J_{1AB}^{(1)} \cos(\pi - \gamma) - J_{2AB}^{(1)} \sin(\pi - \gamma) = -J_{1AB}^{(1)} \cos\gamma - J_{2AB}^{(1)} \sin\gamma \tag{2}$$

where $J_{1AB}^{(1)}$ and $J_{2AB}^{(1)}$ are the two components of the J_k-vector calculated in the local coordinate system $(x_1^{(1)}, x_2^{(1)})$ on segment $\overline{AB}$ in Fig. 1. Since $\overline{AB}$ is traction-free, we have:

$$J_{1AB}^{(1)} = \int_{AB} w n_1^{(1)} \, \mathrm{d}s \tag{3}$$

$$J_{2AB}^{(1)} = \int_{AB} w n_2^{(1)} \, \mathrm{d}s \tag{4}$$

where $n_k^{(1)}$ $(k = 1, 2)$ are the components of the unit outward normal vector to the segment $\overline{AB}$ (Fig. 1).

Now, since $n_1^{(1)} = 0$ but $n_2^{(1)} = 1$ in the $(x_1^{(1)}, x_2^{(1)})$ system, Eq. (3) and hence the first term on the right-hand side of Eq. (2) vanishes. However, Eq. (4), i.e., the second term in (2) does not, given instead by:

$$J_{2AB}^{(1)} = \int_A^B w \, \mathrm{d}s = \frac{1}{\overline{E}} \int_B^A (\sigma_{11}^{(1)})^2 \, \mathrm{d}x_1^{(1)} \tag{5}$$

where $\mathrm{d}s = -\mathrm{d}x_1^{(1)}$ (Fig. 1) has been used, and $\overline{E} = E$ for plane stress and $E/(1 - \nu^2)$ for plane strain, with E and ν representing the Young's modulus and Poisson's ratio, respectively. Apparently, the normal stress $\sigma_{11}^{(1)}$ parallel to segment $\overline{AB}$ contributes to $J_{2AB}^{(1)}$. As pointed out by Herrmann and Herrmann (1981), $\sigma_{11}^{(1)}$ in general does not vanish even though the surface of $\overline{AB}$ is traction-free. Consequently, the second component of the $J_k^{(1)}$-vector evaluated in the local coordinate system along $\overline{AB}$ has non-zero contribution to J_{AB} in Eq. (2). Moreover, different choices of $\overline{AB}$ will generate different contributions to J.

For segment $\overline{DC}$ on the lower surface of the notch, the following result holds:

$$J_{DC} = J_{1DC}^{(2)} \cos\gamma - J_{2DC}^{(2)} \sin\gamma \tag{6}$$

where

$$\begin{aligned} J_{1DC}^{(2)} &= 0 \\ J_{2DC}^{(2)} &= \frac{1}{\overline{E}} \int_D^C (\sigma_{11}^{(2)})^2 \, \mathrm{d}s = \frac{1}{\overline{E}} \int_C^D (\sigma_{11}^{(2)})^2 \, \mathrm{d}x_1^{(2)} \end{aligned} \tag{7}$$

Here, the superscript (2) refers to quantities associated with the local coordinate system $(x_1^{(2)}, x_2^{(2)})$, and $\mathrm{d}s = -\mathrm{d}x_1^{(2)}$, as shown in Fig. 1. Again, different selections of segment $\overline{DC}$ will lead to different and, generally speaking, non-zero contributions to J_{DC}.

More importantly, J_{AB} in Eq. (2) is negative since $J_{2AB}^{(1)}$ in (5) is positive, whereas J_{DC} of (6) is also negative since $J_{2DC}^{(2)}$ of (7) is positive. Thus, J_{AB} and J_{DC} do not cancel each other, even though the remote loading is symmetrical with $\sigma_{12}^{\infty} = 0$ (Fig. 1).

In order to further clarify the situation, the values of J evaluated along three different paths Γ_1, Γ_2 and Γ_3 are compared. It is straightforward to show that:

$$J_{\Gamma 1} + J_{BA} - J_{\Gamma 2} + J_{CD} = 0 \tag{8a}$$

or, equivalently:

$$J_{\Gamma 1} = J_{\Gamma 2} + (J_{AB} + J_{DC}) \tag{8b}$$

Since the sum $J_{AB} + J_{DC}$ does not vanish, it follows that:

$$J_{\Gamma 1} \neq J_{\Gamma 2} \tag{9}$$

We have therefore proved that the J-integral is path-dependent in V-shaped notch problems. In addition, for path Γ_3, the segments $\overline{AH}$ and $\overline{CF}$ have different lengths, and:

$$J_{\Gamma 2} = J_{\Gamma 3} - (J_{AH} + J_{FC}) \tag{10}$$

Due to the different contributions induced from J_2 along the two segments $\overline{AH}$ and $\overline{CF}$, the bracketed term in (10) does not vanish except in the limit when $\gamma = 0$. It is therefore clear that J depends also on the selection of the starting and ending points of the path on the upper and lower surfaces of the notch. Indeed, these contributions are dependent on the selection of points F and H as well as points A and C, resulting in:

$$J_{\Gamma 2} \neq J_{\Gamma 3} \tag{11}$$

The above results reveal that for a V-shaped notch, the path-independence of J is conditional, and hence must be dealt with cautiously. Only when the surfaces of the notch are parallel to its geometrical symmetry line, i.e., the x_1-axis, with $\gamma = 0$ (i.e., a U-shaped notch), could the contributions induced from notch surfaces to J vanish. In other words, only when the projected values of the second component of the J_k-vector defined in the local systems $(x_1^{(1)}, x_2^{(1)})$, or $(x_1^{(2)}, x_2^{(2)})$, do not contribute to J defined in the global system (x_1, x_2) could the value of J be independent of the selection of the starting and ending points on the notch surfaces for the closed contour.

The above manipulations further reveal that the second component of the J_k-vector plays an important role. Therefore, for traction-free surfaces, attention should be focused on this component in local systems and its contribution to J in the global system.

Let us revisit the configuration shown in Fig. 1. The non-trivial contribution induced from the arc $\overset{\frown}{DEB}$ to J can be estimated in a way analogous to that for straight segments, and hence will not be repeated below. However, it should be pointed out that the contribution of $\overset{\frown}{DEB}$ to J does not vanish even if the notch has surfaces parallel to the x_1-axis (i.e., the U-shaped notch), and this conclusion still holds even under pure Mode I loading with $\sigma_{12}^{\infty} = 0$. Furthermore, when the normal stress parallel to the tangential direction at any point on the arc $\overset{\frown}{DEB}$ becomes large due to stress concentration near the notch root, its contribution to J is also likely to be large. The contribution induced from the whole arc may therefore yield considerable errors in J-integral applications, e.g., the R curve evaluation, as demonstrated in the next section.

3. Notch root contribution: numerical examples

To support the above conclusions, numerical calculation is needed to quantify the contribution induced from the whole arc $\overset{\frown}{DEB}$ at the notch root (Fig. 1). For simplicity, a circular arc with radius R is assumed. The contribution of the arc to J is

$$\begin{aligned} J_{\text{arc}} &= -\frac{1}{\overline{\overline{E}}} \int_{-\zeta/2}^{\zeta/2} [\sigma_{11}^{(3)}(\theta)]^2 R \sin\phi \, \mathrm{d}\theta = -\frac{1}{\overline{\overline{E}}} \int_{-\zeta/2}^{\zeta/2} [\sigma_{11}^{(3)}(\theta)]^2 R \sin(\pi/2 + \theta) \, \mathrm{d}\theta \\ &= \frac{1}{\overline{\overline{E}}} \int_{-\zeta/2}^{\zeta/2} \left[\sigma_{11}^{(3)}(\theta)\right]^2 R \cos\theta \, \mathrm{d}\theta \end{aligned} \tag{12}$$

where the angles ϕ and θ are defined in Fig. 1, $\sigma_{11}^{(3)}(\theta)$ refers to the normal stress component along the tangential direction on the surface of the circular arc defined in a local coordinate system $(x_1^{(3)}, x_2^{(3)})$, $\zeta = \pi$ for a U-shaped notch, and $\zeta = \pi - 2\gamma$ for a V-shaped notch.

Note that the integrand in (12) is an even function of θ so that the integral J_{arc}, generally speaking, does not vanish. In other words, the contribution induced from the upper half arc and that from the lower half arc do not cancel each other even if the far-field loading is symmetrical with $\sigma_{12}^{\infty} = 0$; rather, the two contributions add to yield the total contribution from the arc. Therefore, Eq. (12) has provided a clear evidence on the non-zero contribution from the notch root to J. The total J of the notch is the sum of J_{arc} and the J-integral along a path away from the notch root that does not contain any of the notch surfaces (e.g., path Γ_2 or Γ_3 in Fig. 1).

To calculate J_{arc}, one needs to know the detailed distribution of stress component $\sigma_{11}^{(3)}(\theta)$ along the arc $\overset{\frown}{DEB}$ (Fig. 1). This component is related to stresses σ_{11}, σ_{12}, σ_{22} defined in the global system (x_1, x_2) by:

$$\sigma_{11}^{(3)}(\theta) = \sigma_{11}\cos^2\phi + 2\sigma_{12}\sin\phi\cos\phi + \sigma_{22}\sin^2\phi \tag{13}$$

where $\phi = \pi/2 + \theta$. Although there have been numerous investigations on notch problems, most focus either on stress concentration just ahead of the notch or on a small crack initiating from the notch root due to fatigue. However, the illuminating work of Lazzarin and Tovo (1996) and Lazzarin et al. (1998) does provide an analytical solution with first order approximation for near-notch surface stresses. For completeness, a concise summary of stress distribution near the notch root is given in Appendix A.

Two scenarios are considered: $\gamma = 0°$ and $\gamma = 15°$ (Fig. 1), corresponding to a U-shaped notch and a V-shaped notch, respectively. The parameters associated with the first order approximation of Lazzarin and Tovo (1996) are calculated as:

$$r_0 = R/2, \quad \lambda = 0.5, \quad \chi = 1.0, \quad \mu = -0.5 \tag{14a}$$

for $\gamma = 0°$, and

$$r_0 = R/2.2, \quad \lambda = 0.5015, \quad \chi = 1.0710, \quad \mu = -0.4239 \tag{14b}$$

for $\gamma = 15°$. The definitions of r_0, λ, χ and μ are given in Appendix A. The maximum stress at the notch tip is linked to a field parameter K_1^* by means of notch root radius and opening angle 2γ (implicitly via r_0 and λ, respectively):

$$\sigma_{\max} = \frac{4K_1^* r_0^{\lambda-1}}{\sqrt{2\pi}[(1+\lambda) + \chi(1-\lambda)]} \tag{15}$$

where

$$K_1^* = \sqrt{2\pi}\operatorname*{Lim}_{R\to 0}(\sigma_\theta)_{\theta=0}R^{1-\lambda} \tag{16}$$

Here, σ_θ is the hoop stress, and K_1^* represents a field parameter proportional to the remote stress σ_{22}^{∞}, which degenerates in the case of $R = 0$ and $\gamma = 0$ to the conventional stress intensity factor K_1 (Gross and Mendelson, 1972). When SI units are adopted, the length parameters such as the notch root radius R are expressed in meters, the stresses σ_{22}^{∞} and $\sigma_{\max}$ as well as the Young's modulus $\overline{E}$ are in MPa, and the J-integral is in MN/m, respectively. For a U-shaped notch with zero opening angle, the ratio $\sigma_{\max}/K_1^*$ has unit $m^{-0.5}$. On the other hand, for a V-shaped notch with an opening angle $2\gamma = 30°$, the unit of $\sigma_{\max}/K_1^*$ is $m^{-0.4986}$. The difference between these two kinds of notches is therefore small for the purpose of engineering design, but physically this fact should be highlighted especially when the notch root ratio R tends to zero. This is because the solution of Lazzarin and Tovo (1996) is only a first order approximation. Consequently, it is unclear whether the parameters $(r_0, \lambda, \chi, \mu)$ associated with the first order approximation remain

unchanged as the notch root ratio R tends to zero. In other words, only if $\sigma_{\max}/K_1^*$ has unit $m^{-0.5}$ will K_1^* be considered as the conventional stress intensity factor.

According to Gross and Mendelson (1972), a natural expression of the normalized J-integral for U- and V-shaped notches is

$$J_{\text{arc}} = \frac{Y}{\overline{E}} R \left[\frac{K_1^*}{\delta R^{1-\lambda 1}} \right]^2 \tag{17a}$$

where Y is a non-dimensional parameter introduced for numerical analysis, the subscript arc refers to the quantity contributed by the notch arc only, and $\delta R^{1-\lambda 1}$ is introduced by Gross and Mendelson (1972) as:

$$K_1^* = \delta R^{1-\lambda 1} \sigma_{\max} \tag{17b}$$

Thus, upon suitable coordinate transformation and substitution of Eq. (A.5) into (13) and subsequently into (12), the normalized value of the J-integral induced from the projected value of the J_2-integral evaluated along the whole arc, with θ ranging separately from $-\pi/2$ to $\pi/2$ for a U-shaped notch and from $-5\pi/12$ to $5\pi/12$ for a V-shaped notch, is given by:

$$J_{\text{arc}} = \frac{Y}{\overline{E}} \{\sigma_{\max}\}^2 R \tag{17c}$$

After calculating the contribution of the notch arc to J_{arc}, it is found that $Y = 0.5453$ for the U-notch and 0.5004 for the V-notch ($\gamma = 15°$). It is worth mentioning that Y is dependent of the notch opening angle γ, but not the notch root radius R. It is emphasized here that Y is independent of R because, in the present case where the solid is infinitely large, there is no other length scale that can be used to normalize R. This conclusion is no longer valid for a finite notch in a finite plane solid, which can be solved using, say, the finite element method (FEM). In other words, the numerically calculated values of Y in (17a,c) will be different if different lengths of the finite notch, say a, are used to normalize the root radius R. It is expected, however, that in the limit when $R/a \to 0$, Y will approach a constant, e.g., 0.5453 for a U-notch.

It is intriguing to note that the Y value for a U-notch is larger than that for a V-notch under the same remote loading conditions. However, it should be emphasized that Eq. (17a) or (17c) does not account for the contribution of the upper and lower straight lines of the V-notch, and that the calculation for the U-notch is performed from $-\pi/2$ to $\pi/2$ and for the V-notch from $-5\pi/12$ to $5\pi/12$ ($\gamma = 15°$). Again, this conclusion is no longer valid for a finite notch in a finite plane solid, which can be solved with FEM if the numerically calculated values of Y in (17a,c) contain the contribution induced from the upper and lower straight lines for the V-shaped notch. The predicted J_{arc} values are listed in Table 1 for a U-shaped notch with $r_0/R = 0.5$; the following cases are considered: $r_0 = 0.125$, $R = 0.25$; $r_0 = 0.25$, $R = 0.5$; $r_0 = 0.5$, $R = 1.0$; $r_0 = 0.75$, $R = 1.5$; $r_0 = 1.00$, $R = 2.00$; $r_0 = 1.25$, $R = 2.50$; $r_0 = 1.50$, $R = 3.00$; $r_0 = 1.75$, $R = 3.50$; and $r_0 = 2.00$, $R = 4.00$. Similarly, Table 2 presents the predicted values of J_{arc} for a V-shaped notch with $r_0/R = 0.4545$; the following cases are considered: $r_0 = 0.125$, $R = 0.275$; $r_0 = 0.25$, $R = 0.55$; $r_0 = 0.500$, $R = 1.100$; $r_0 = 0.750$, $R = 1.650$; $r_0 = 1.00$, $R = 2.200$; $r_0 = 1.25$, $R = 2.75$; $r_0 = 1.50$, $R = 3.30$; $r_0 = 1.75$, $R = 3.85$; and $r_0 = 2.00$, $R = 4.4$. The numerical results of Tables 1 and 2 not only confirm our calculations but also confirm the independence feature of Y.

Table 1
Normalized values of J_{arc} for a U-shaped notch with root ratio $r_0/R = 0.5$

r_0/R	$Y = \frac{J_{\text{arc}}\overline{E}}{R(\sigma_{\max})^2}$	$\frac{\sqrt{R}\sigma_{\max}}{K_1^*}$
0.5	0.5453	1.128

Table 2
Normalized values of J_{arc} for a V-shaped notch with root ratio $r_0/R = 0.4545$

r_0/R	$Y = \frac{J_{arc}\overline{E}}{R(\sigma_{max})^2}$	$\frac{\sqrt{R}\sigma_{max}}{K_1^*}$
0.4545	0.5004	0.7852

Note that, for a fixed notch root radius, the J-integral associated with a U-shaped notch is always larger than that associated with a V-shaped notch. This implies that the arc of the U-shaped notch yields more contribution to J than that of the V-shaped notch, for two reasons. Firstly, the upper and lower integration limits in (12) for the V-notch, $\pm(\pi/2 - \gamma)$, are smaller than those for the U-notch, $\pm\pi/2$. Secondly, whilst the straight surfaces of the U-notch are parallel to the x_1-axis and hence yield no contribution to J, the inclined surfaces of the V-notch have non-zero contributions to the J. As the calculation of the contributions induced from the two inclined surfaces requires not only detailed knowledge on the distribution of normal stress along the tangential direction of the surfaces but also integration over an infinite interval yet to be determined, it is deemed beyond the scope of this paper.

Again, it should be emphasized that although the Y values listed in Table 2 are independent of R, this conclusion cannot be extrapolated to a finite V-shaped notch in a finite plane solid. For both U- and V-shaped notches, Y is a function of R/a, with Y approaching asymptotically a constant when $R/a \to 0$.

4. Discussion

Eqs. (17a) or (17c) provides a fundamental understanding of the J-integral analysis in situations where inclined or curved traction-free surfaces are concerned. The necessary conditions under which J is path-independent have been clarified in detail, which is of significance in practical applications of the integral. Of great interest is that numerical results of the normalized J-integral are independent of the notch root radius R (or r_0) for a U-notch (Table 1), and are insensitive to variations in R for a V-notch (Table 2). These results are actually expected, which not only validate the present calculations, but also confirm the analytical formulations presented by Lazzarin and Tovo (1996) and Lazzarin et al. (1998). The explanation lies in the fact that the root radius of a semi-infinite notch (rather than a notch of finite length) could not be said as large or small, since there is no other length scale in Fig. 1 that may be used for comparison. Of course, for a finite notch in a finite solid, different radii of the notch would lead to different values of the Y-factor.

By comparing (17a,c) with the traditional formula of J in terms of stress intensity factor for a semi-infinite sharp crack having the well-known inverse square root singularity, it can be seen that there actually exists a new factor, denoted here by Y, which represents the divergence of J contributed by a notch containing an arc at the root from that contributed by a plane crack. Obviously, different shapes of the arc at the notch root will yield different values of the Y factor; the external geometrical configuration and loading condition will also influence Y.

Another expected result is that the J-integral for a plane crack is always larger than that of a notch having the same length as that of the crack.

Thus, an intriguing question arises as to why previous researchers have encountered little, if any, difficulty in measuring J from, say, the widely used compact tension (CT) specimens. The main reason is that these experimental studies are mostly based on the compliance technique built upon the principle of minimal potential energy. For two-dimensional notch problems, the J-integral, in its energy release rate form, is given by (Kanninen and Popelar, 1985):

$$J = -\mathrm{d}\Pi/\mathrm{d}a \tag{18}$$

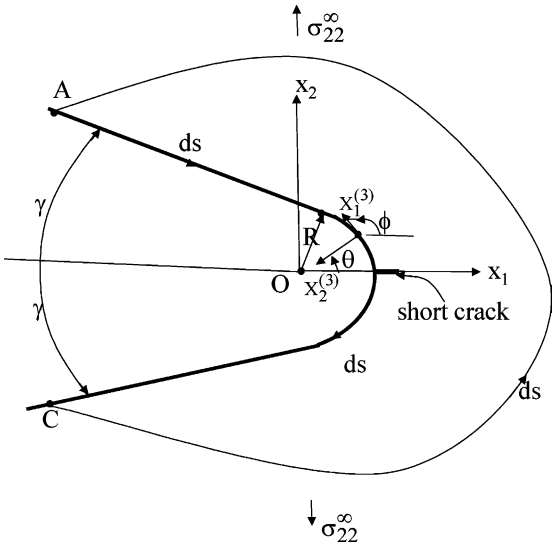

Fig. 2. Short crack in front of a notch root.

where da denotes the change in notch length and dΠ refers to the corresponding change in potential energy Π for a given notch configuration. Eq. (18) leads to a finite difference method for obtaining approximate values of J using the small deformation theory (see, e.g. Rice, 1968b; Ranaweera and Leckie, 1982; Kanninen and Popelar, 1985). The compliance method has been well demonstrated, even for generalized non-linear elastic power-law hardening materials, with:

$$J \approx -[\Pi(a + \Delta a) - \Pi(a)]/\Delta a \tag{19}$$

where Δa should be much smaller than the original notch length a (for example, Δa has been customarily chosen as $\Delta a = 0.001a$).

The conclusions reached in this paper are in fact not at odds with the widely recognized compliance technique, because the J-integral measured from (19) has implicitly included the contribution induced from the projected values of the J_2-integral along notch surfaces as well as the arc at the notch root. However, because J is sensitive to the geometrical configuration of the notch, this may explain why there is large scatter in the toughness and fatigue data measured by different researchers for nominally identical materials.

Finally, in situations where a short crack has initiated from the notch tip E (see Fig. 2), the stress concentration is released by the formation of the short crack. However, the conclusions reached above should still hold although detailed stress distributions along the arc bisected by the crack are expected to be quite different from those derived by Lazzarin and Tovo (1996). The contribution to J induced from the arc cut by the crack should be much smaller that those listed in Tables 1 and 2 due to the release of stress concentration near the notch root. For brevity, however, this topic will not be elaborated further.

5. Conclusion

Based on the results presented in this paper, the following conclusions can be drawn:

(1) A new condition that restricts the path-independence of the J-integral is obtained. That is, the projected contributions from the J_2-integral evaluated in local coordinate system along the integration path

(traction-free surfaces) must vanish in order to ensure the path-independence of J. For a V-notch, J is path-dependent and its value is dependent upon the selection of the starting and ending points on notch surfaces, even though these surfaces are traction-free. This conclusion is valid even if the V-notch is subjected to a loading symmetrical with respect to its geometrical symmetrical line. For a U-notch, the path-independence of J is ensured as the projected values induced from the J_2-integral vanish, subject to the condition that the selected integration path encloses completely the notch root. However, it should be emphasized that, for both types of notch, the arc at the notch root always contributes to J, even under remote symmetrical loadings.

(2) The J-integral induced from a notch with an arc at its root has a value that is always less than that from a sharp crack under the same geometrical and loading conditions. This means that the formation of a sharp crack releases more potential energy than the formation of a notch.
(3) The second component of the J_k-vector, J_2, plays an important role in studying fracture of notch-like defects. This component should bring more attention in future investigations.
(4) Adequate studies are needed to quantify the errors associated with the path-independence assumption of J when evaluating R-curves from notch specimens.

Acknowledgements

This work is supported partly by a Royal Society Fellowship Award for YHC's visit to Cambridge University, partly by the Teng-Fei program for TJL's visit to Xi'an Jiaotong University, and partly by the National Natural Science Foundation of China. The authors wish to thank the critical comments given by the reviewers on the original manuscript.

Appendix A. Stress distribution near a notch root

The global Cartesian coordinate system (X, Y) used by Lazzarin and Tovo (1996) is slightly different from the (x_1, x_2) system shown in Fig. 1. The two systems are related to each other by

$$\begin{aligned} X &= x_1 - (R - r_0) \\ Y &= x_2 \end{aligned} \tag{A.1}$$

where R is the radius of the arc and r_0 is the distance between the origin of (X, Y) and the notch root. Similarly, from Eq. (A.1), the polar coordinates (ρ, ϑ) used by Lazzarin and Tovo (1996) are related with (r, θ) in Fig. 1 by

$$\begin{aligned} \rho &= \sqrt{(x_1 - R + r_0)^2 + x_2^2} \\ \vartheta &= \tan^{-1}(x_2/(x_1 - R + r_0)) \end{aligned} \tag{A.2}$$

where

$$\begin{aligned} r &= \sqrt{x_1^2 + x_2^2} \\ \theta &= \tan^{-1}(x_2/x_1) \end{aligned} \tag{A.3}$$

The following coordinate transformation is introduced by Lazzarin and Tovo (1996):

$$Z = x_1 + \mathrm{i}x_2 = w^q = (u + \mathrm{i}v)^q \tag{A.4}$$

where Z and w are complex, $\mathrm{i} = \sqrt{-1}$, q is an exponent depending on the shape of the notch, and (u, v) represent a new curvilinear system with $u = 0$ denoting a sharp notch and $u = \text{constant} > 0$ denoting the

traction-free surface of a blunt notch. By introducing a first order approximation, Lazzarin and Tovo (1996) then obtained the following stress components:

$$\begin{Bmatrix} \sigma_\vartheta \\ \sigma_\rho \\ \sigma_{\rho\vartheta} \end{Bmatrix} = \frac{\sigma_{\max}}{4}\left(\frac{\rho}{r_0}\right)^{\lambda-1}\left(\begin{Bmatrix} (1+\lambda)\cos(1-\lambda)\vartheta \\ (3-\lambda)\cos(1-\lambda)\vartheta \\ (1-\lambda)\sin(1-\lambda)\vartheta \end{Bmatrix} + \chi(1-\lambda)\begin{Bmatrix} \cos(1+\lambda)\vartheta \\ -\cos(1+\lambda)\vartheta \\ \sin(1+\lambda)\vartheta \end{Bmatrix} + \left(\frac{\rho}{r_0}\right)^{\mu-\lambda}[(3-\lambda)-\chi(1-\lambda)]\begin{Bmatrix} \cos(1+\mu)\vartheta \\ -\cos(1+\mu)\vartheta \\ \sin(1+\mu)\vartheta \end{Bmatrix}\right) \tag{A.5}$$

where

$$\begin{aligned} &2\alpha = \pi(2-q) \\ &R = qr_0/(q-1) \end{aligned} \tag{A.6}$$

The three constants λ, μ, χ in (A.5) are determined by:

$$\begin{aligned} &\sin(\lambda q\pi) + \lambda\sin(q\pi) = 0 \\ &\mu = 1/q - 1 - \left\{\frac{[(1-\lambda)^2 - (1+\lambda)/q] + \chi(1-\lambda)[(1+\lambda) - 1/q]}{(3-\lambda)-\chi(1-\lambda)}\right\} \\ &\chi = -\sin[(1-\lambda)q\pi/2]/\sin[(1+\lambda)q\pi/2] \end{aligned} \tag{A.7}$$

With $2\gamma = 30°$ for a typical V-notch (ASTM, 1990), $q = 11/6 \approx 1.8333$. For a U-notch with $2\gamma = 0°$, $q = 2$. Thus, from (A.6), $R = 2r_0$ for a U-notch and $R = 2.2r_0$ for a V-notch with $2\gamma = 30°$. The corresponding values for λ, μ, χ are listed in Eqs. (14a) and (14b) of Section 3.

Upon substituting λ, μ, χ into (A.5) and then into (12) and (13), a numerical integration could be performed to calculate the contribution to J induced from a U-notch and a V-notch, respectively. The well-known Chebyshev numerical scheme is adopted to carry out the integration in Eq. (12) with desired accuracy.

References

ASTM Standards, 1990. Vol. 03.01, pp. 812–822.

Atluri, S.N., 1982. Path independent integrals in finite elasticity and inelasticity, with body forces, inertia, and arbitrary crack-face conditions. Engineering Fracture Mechanics 18, 341–364.

Atzori, B., Lazzarin, P., Tovo, R., 1997. Stress distributions for V-shaped notches under tensile and bending loading. Fatigue and Fracture of Engineering Materials and Structures 20, 1083–1092.

Blackburn, W.S., 1972. Path independent integral to predict onset of crack instability in an elastic–plastic material. International Journal of Fracture 8, 343–346.

Blackburn, W.S., Jack, A.D., Hellen, T.K., 1977. An integral associated with state of a crack tip in a non-elastic material. International Journal of Fracture 13, 183–200.

Batte, A.D., Blackburn, W.S., Elsender, A., Hellen, T.K., Jackson, A.D., 1983. A comparison of the J-integral with other methods of post yield fracture mechanics. International Journal of Fracture 21, 46–66.

Budiansky, B., Rice, J.R., 1973. Conservation laws and energy-release rates. ASME Journal of Applied Mechanics 40, 201–203.

Castro, P.M.S.T., 1982. Comparison of J testing techniques and correlation J-COD using structural steel specimens. International Journal of Fracture 17, 83–96.

Chen, Y.H., Hasebe, N., 1998. A consistency check for strongly interacting multiple crack problem in isotropic, anisotropic, and bimaterial solids. International Journal of Fracture 89, 333–353.

Elhaddad, M.H., Dowling, N.E., Topper, T.H., Smith, K.N., 1980. J-integral applications for short fatigue cracks at notches. International Journal of Fracture 16, 15–30.

Eshelby, J.D., 1970. The energy momentum tensor in continuum mechanics, in: Kanninen, M.F. et al. (Eds.), Inelastic Behavior of Solids. McGraw-Hill, New York.

Glinka, G., Newport, A., 1987. Universal features of elastic notch-tip stress fields. International Journal of Fatigue 9, 143–150.

Gross, D., Mendelson, A., 1972. International Journal of Fracture Mechanics 8, 267–276.

Herrmann, A.G., Herrmann, G., 1981. On energy release rates for a plane crack. ASME Journal of Applied Mechanics 48, 525–530.

Hutchinson, J.W., 1979. Nonlinear Fracture Mechanics, Department of Solid Mechanics, The Technical University of Denmark.

Kanninen, M.F., Popelar, C.F., 1985. Advanced Fracture Mechanics. Oxford University Press, New York.

Knowles, J.K., Sternberg, E., 1972. On a class of conservation laws in linearized and finite elastostatics. Archive for Rational Mechanics and Analysis 44, 187–211.

Kujawski, D., 1991. Estimations of stress intensity factors for small cracks at notches. Fatigue and Fracture of Engineering Materials and Structures 14, 953–965.

Kujawski, D., Shin, C.S., 1997. On the elastic longitudinal stress estimation in the neighborhood of notches. Engineering Fracture Mechanics 56, 137–138.

Lazzarin, P., Tovo, R., 1996. A unified approach to the evaluation of linear elastic fields in the neighbourhood of cracks and notches. International Journal of Fracture 78, 3–19.

Lazzarin, P., Tovo, R., Filippi, S., 1998. Elastic stress distributions in the finite size plates with edge notches. International Journal of Fracture 91, 269–282.

McMeeking, R.M., 1980. ASTM STP 631, pp. 28–41.

Ranaweera, M.P., Leckie, F.A., 1982. *J*-integrals for some crack and notch geometries. International Journal of Fracture 18, 3–18.

Rice, J.R., 1968a. A path independent integral and the approximate analysis of strain conservation by notches and cracks. ASME Journal of Applied Mechanics 35, 379–386.

Rice, J.R., 1968b. Mathematical analysis in the mechanics of fracture, in: Liebowitz, H. (Ed.), Fracture, vol. II. Academic Press, New York, pp. 191–308.

Shin, C.S., Man, K.C., Wang, C.M., 1994. A practical method to estimate the stress concentration of notches. International Journal of Fatigue 16, 242–255.

Sinclair, G.B., Mullan, D., 1982. A simple yet accurate finite element procedure for computing stress intensity factors. International Journal of Fatigue 18, 1587–1600.

Sinclair, G.B. et al., 1984. path independent integrals for computing stress intensity factors at sharp notches in elastic plates. International Journal for Numerical Methods in Engineering 20, 999–1008.

Xu, R.X., Thompson, J.C., Topper, T.H., 1995. Practical stress expressions for stress concentration region. Fatigue and Fracture of Engineering Materials and Structures 18, 885–895.